

Dielectric properties of $(1-x)\text{La}(\text{Mg}_{1/2}\text{Ti}_{1/2})\text{O}_3-x\text{SrTiO}_3$ ceramicsM.P. Seabra^a, A.N. Salak^a, V.M. Ferreira^{a,*}, J.L. Ribeiro^b, L.G. Vieira^b^aDepartment of Ceramics and Glass Engineering/CICECO, University of Aveiro, 3810-193 Aveiro, Portugal^bDepartment of Physics, University of Minho, 4710-057 Braga, Portugal

Received 20 July 2003; accepted 4 October 2003

Abstract

Powders of $(1-x)\text{La}(\text{Mg}_{1/2}\text{Ti}_{1/2})\text{O}_3-x\text{SrTiO}_3$ series have been prepared by a non-conventional chemical route based on the Pechini method. Homogeneous solid solutions allowed the sintering of dense and single-phase ceramics for the full composition range ($0 \leq x < 1$). Crystal structure of the ceramics was investigated by XRD and several compositional driven structural transformations were observed. The dielectric function of the ceramics was measured at radio, microwave and far infrared (FIR) frequency ranges to help clarifying the relationship between dielectric properties and structure. The FIR data were found to reflect clearly the sequence of structural modifications observed. In order to evaluate the importance of intrinsic mechanisms in the dielectric response at the GHz and MHz ranges, the reflectivity spectra were fit to the Berreman–Unterwald form of dielectric function. The fits showed that the lower frequency dielectric response seems to be dominated by lattice phonons. Microwave permittivity and temperature coefficient of the resonant frequency were found to obey a hyperbolic-type law.

© 2003 Elsevier Ltd. All rights reserved.

Keywords: Dielectric properties; $\text{La}(\text{Mg,Ti})\text{O}_3$; Perovskites; Powders-chemical preparation; Spectroscopy; SrTiO_3

1. Introduction

Wireless telecommunications is perhaps the sector of electronic industry showing the more dramatic growth in the past two decades. The use of ceramic materials in the fabrication of modern high-frequency filters and resonators has stimulated the search for new low-cost materials for technological applications. The improvement of dielectric materials has been focused on the tailoring of systems showing high unloaded quality factors (Q), high dielectric permittivity (ϵ') and near zero temperature coefficients of the resonant frequency (τ_f), because these qualities are necessary to decrease the size of the devices and assure the frequency stability and selectivity of the components under different atmospheric conditions.¹ Nevertheless to achieve these requirements it is usually necessary to reach a compromise.

$\text{La}(\text{Mg}_{1/2}\text{Ti}_{1/2})\text{O}_3$ (LMT) is a promising complex perovskite that displays a high value of $Q \times f$ (114 000 GHz; f represents the resonance frequency) and a moderate

value of permittivity ($\epsilon' = 27$). Its main drawback is the relatively high magnitude of the temperature coefficient of resonant frequency τ_f (−81 ppm/K).² In principle, the tuning of τ_f to near-zero values may be achieved by the formation of solid solutions with other compounds having coefficients τ_f of opposite sign. Earth alkaline titanates, that usually present high positive τ_f and high permittivity, appear as natural candidates. Among them, incipient ferroelectric SrTiO_3 (ST) seems adequate because has, at the microwave range, a high dielectric permittivity ($\epsilon' = 290$), a moderate $Q \times f$ value (4800 GHz) and a high and positive τ_f (+1600 ppm/K).³

The ability of LMT and ST to form homogeneous solid solutions has been previously investigated.⁴ The structure of LMT is monoclinic ($\text{P}2_1/n$, $z=4$) and is characterized by both in-phase and anti-phase tilting of the oxygen octahedra, La displacement and high degree of Mg/Ti ordering. The increase of the ST content in the solid solution induce a sequence of structural transformations [$\text{P}2_1/n \Rightarrow \text{Pbnm} \Rightarrow \text{Imma} \Rightarrow \text{I}4/\text{mcm} \Rightarrow \text{Pm}3\text{m}$] that are related to the loss of B-site cation order, La/Sr anti-parallel displacement and modifications of the octahedral tilting.⁴

* Corresponding author. Tel.: +351-234-370354; fax: +351-234-425300.

E-mail address: victorf@cv.ua.pt (V.M. Ferreira).

This work reports on the dielectric properties of $(1-x)\text{LMT}-x\text{ST}$ system and aims to help establishing their relation to the structural modifications observed. To this purpose, the dielectric response of the material has been studied as a function of the composition at radio, microwave and far infrared (FIR) frequency ranges.

2. Experimental

$(1-x)\text{LMT}-x\text{ST}$ ceramics ($0 \leq x < 1$) have been prepared by using powders obtained by a chemical route based on the Pechini method, previously optimized for LMT.⁵ In order to achieve the highest possible density, pellets with 10 mm in diameter and about 1 mm in thickness were isostatically pressed at 200 MPa into discs and sintered in air for 2 h at temperatures ranging between 1770 and 1870 K (depending on composition). For the compositions with $0 \leq x \leq 0.5$ high densities ($> 95\%$) were attained by sintering the pellets at 1870 K during 2 h. In the case of $x = 0.7$, a lower sintering temperature (1770 K) was used to achieve the same degree of densification. For $x = 0.9$ different sintering conditions (temperature and atmosphere) were tried, but the degree of densification achieved was always close but lower than 95%. The chemical homogeneity of the samples was systematically analyzed by energy dispersive spectroscopy (EDS). For scanning electron microscopy (SEM) (Hitachi S-4100) the samples were polished to a 1 μm finish and thermally etched 50 K below their optimum sintering temperature for 2 min.

For microwave measurements, the samples were prepared in a cylindrical shape with 10 mm in diameter and 8–10 mm length. The samples for low frequency dielectric measurements were polished to form disks with a thickness of 0.5–0.7 mm, electroded by deposition of platinum and annealed at 1100 K. The samples investigated by FIR reflectivity were prepared as thin slabs with optically polished faces.

The room temperature permittivity, Q -factor and resonant frequency of the different compositions were measured at microwave frequency range by the Hakki–Coleman method,⁶ using a 10 MHz to 20 GHz Scalar Analyzer (IFR 6823). The values of τ_f were evaluated by measuring the variation of the resonant frequency of the samples with temperature, on cooling runs between 230 and 300 K (at a rate of 2 K/min). The measurements were carried out in an oxygen-free cavity of high-conductivity copper, cooled by a CTI Cryogenics model 22 refrigerator with an 8200 compressor, coupled to a Lakeshore 330 Temperature Controller.⁷

The infrared reflectivity measurements were performed with a Brüker IFS-66V spectrometer in the spectral range 40–2000 cm^{-1} . Room temperature pyroelectric detectors of DTGS with PE or KBr windows and 6 μm 8 Mylar or KBr beam-splitters were used in

the FIR and medium IR ranges, respectively. For each composition studied, the IR complex dielectric permittivity was evaluated by fitting the spectra to the factorized form of dielectric function.⁸

The real and imaginary parts of the dielectric function were also measured with a Hewlett Packard Precision LCR meter (HP 4884A) as functions of temperature and frequency in the ranges of 300–550 K (heating rate of 1.5 K/min) and 10^2 – 10^6 Hz, respectively.

3. Results and discussion

Fig. 1 shows typical secondary electron SEM images of polished and thermally etched surfaces of samples with compositions $x = 0, 0.1, 0.3, 0.5$. In all cases, the microstructure is uniform and no traces of second phases were detected. Note that the average grain size of the ceramics increases notably as the content of ST increases. However, this feature does not affect much the dielectric response of $(1-x)\text{LMT}-x\text{ST}$ ceramics. Indeed, detailed studies of grain size effect performed on high-quality dielectric ceramics have revealed that the variation in microwave dielectric loss (ϵ'') or permittivity is negligible when samples are dense.^{9,10}

As previously reported,⁴ the major peaks in the XRD spectra of $(1-x)\text{LMT}-x\text{ST}$ could be indexed according to a simple perovskite structure. However, in all the samples investigated, several additional weak reflections were observed at half integer positions, which indicate that a sequence of tilt transitions occurs as x increases. Table 1 summarizes the nature of the observed composition driven structural modifications. The tilt systems $\text{P2}_1/\text{n}$ (monoclinic) and Pbnm (orthorhombic) are identical ($a^-a^-c^+$), differing only in the presence ($x < 0.3$) or absence ($x \geq 0.3$) of B-site order. For composition $x = 0.7$, the structure is still orthorhombic (Imma) but the in-phase tilt disappears [tilt system ($a^-a^-c^0$)]. For $x = 0.9$ the structure becomes tetragonal (I4/mcm), with only one anti-phase tilt axis ($a^0a^0c^-$).

Fig. 2 displays the infrared reflectivity spectra of the different compositions studied ($0 \leq x \leq 0.7$). As can be seen, the IR spectra reflect the structural transformations, being clear a progressive reduction of the number of active modes as the symmetry increases from monoclinic ($x = 0$, $\text{P2}_1/\text{n}$) to orthorhombic ($x = 0.7$, Imma). Consider first the end members, LMT and ST. For LMT ($z = 4$, $\text{P2}_1/\text{n}$), the factor group analysis¹¹ indicates that the Γ -point normal modes can be decomposed into $(12+3)\text{A}_g + (12+3)\text{B}_g + 17\text{A}_u + 16\text{B}_u$, where the modes numbered in italic correspond to those resulting from the double occupation of the B-site. If the structure of LMT could be approximately described by a double simple perovskite unit cell with a long range ordered B-site occupation ($z = 2$, Fm3m), then one should expect only five triple degenerated Γ -point modes $[(3+1)\text{F}_{1u} + \text{F}_{2u}]$.

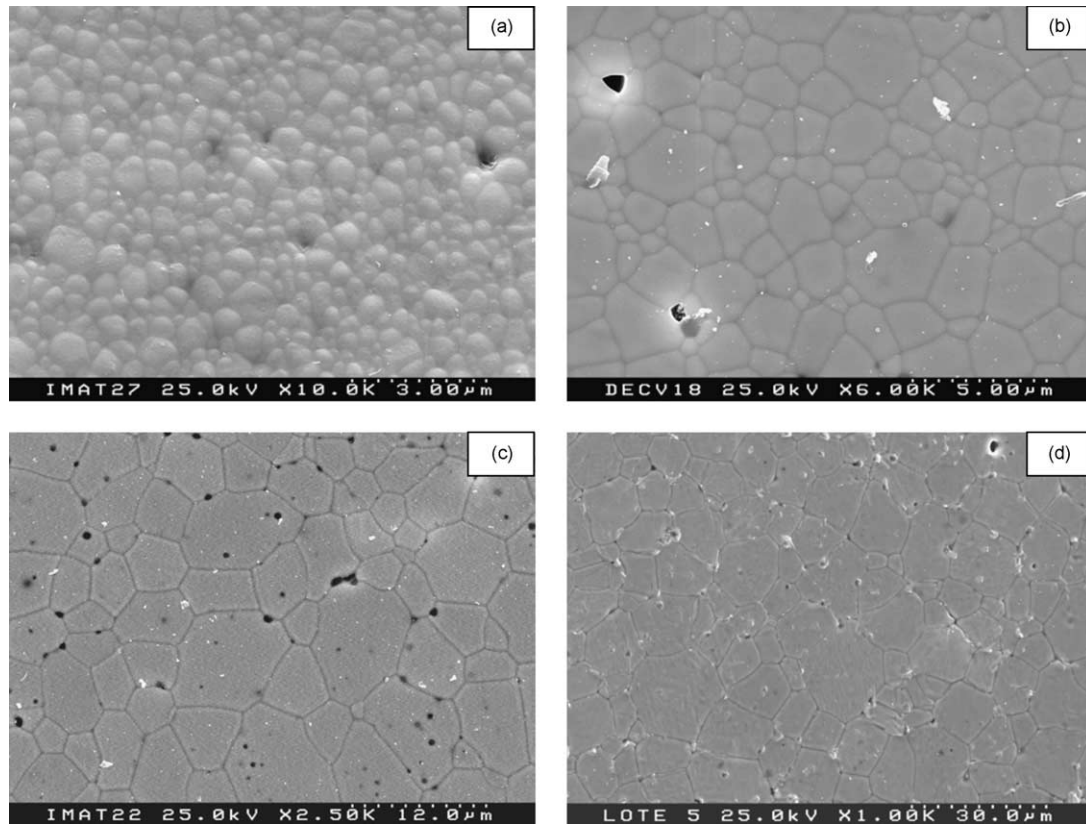


Fig. 1. SEM photographs of polished and thermally etched surfaces of the $(1-x)\text{LMT}-x\text{ST}$ ceramics sintered at 1870 K for 2 h, where $x=0$ (a), 0.1 (b), 0.3 (c) and 0.5 (d).

Table 1
Structural changes in the $(1-x)\text{LMT}-x\text{ST}$ system

Composition	Cation ordering 1/2 (111)	Cation displacement 1/2 (210) 1/2 (300)	In-phase tilting 1/2 (310) 1/2 (321)	Anti-phase tilting 1/2 (311)	Space group
$x \leq 0.1$	x	x	x	x	$\text{P2}_1/\text{n}$
$0.1 < x \leq 0.3$		x	x	x	Pbnm
$0.3 < x \leq 0.5$			x	x	Pbnm
$0.5 < x \leq 0.7$				x	Imma
$0.7 < x \leq 0.9$				x	I4/mcm

For cubic ST ($z=1$, $\text{Pm}3\text{m}$), one should expect four triple degenerated modes [$3\text{F}_{1\text{u}} + \text{F}_{2\text{u}}$], being obviously absent the additional R-mode [$\mathbf{k} = (1/2, 1/2, 1/2)\mathbf{a}^*$] due to the folding of the Brillouin zone and related to the B-B' stretching vibrations. Thus, the number of IR active modes would be 33 for monoclinic LMT ($17\text{A}_{\text{u}} + 16\text{B}_{\text{u}}$) or 4 triply degenerated for a $A(\text{B}_{1/2}\text{B}'_{1/2})\text{O}_3$ ordered perovskite [$(3+1)\text{F}_{1\text{u}}$]. A detailed analysis of the LMT spectrum, both by Kramers–Kronig inversion and by simulation with the factorized form of the dielectric function disclosed 15 active modes, which seems in disagreement with both cases considered above. However, if one takes into account that the anisotropy is effectively averaged out (as is very often the case in ceramic

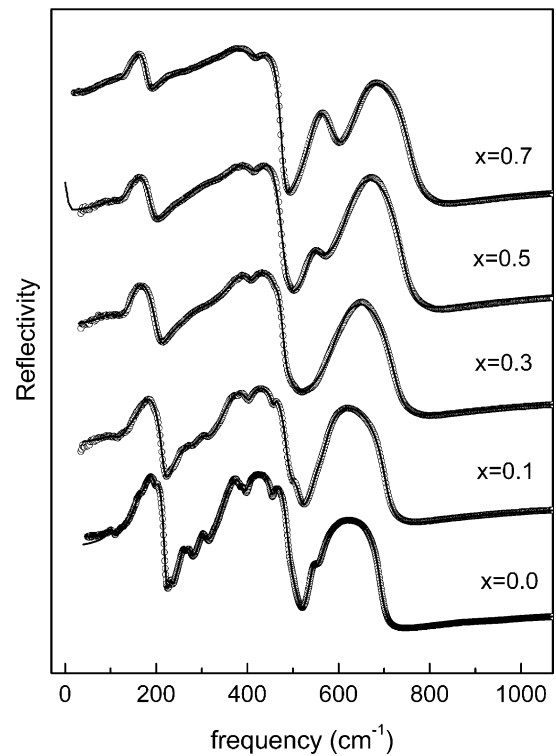


Fig. 2. Infrared reflectivity spectra of the $(1-x)\text{La}(\text{Mg}_{1/2}\text{Ti}_{1/2})\text{O}_3-x\text{SrTiO}_3$ system.

samples), then the modes A_u and B_u cannot be resolved and the number of effective modes for monoclinic LMT should be reduced to 17. The number of modes experimentally detected (15) is therefore compatible with the monoclinic symmetry observed by XRD. In the case of the solid solutions with a orthorhombic structure (e.g. $x=0.5$, $z=4$, Pbnm), the number of modes detected is eight and factor group analysis indicates the decomposition $7A_g + (8+3)A_u + 7B_{1g} + (8+3)B_{1u} + 5B_{2g} + (10+3)B_{2u} + 5B_{3g} + (10+3)B_{3u}$. Hence, if the anisotropy of the spectra is averaged out and is assumed that the modes related to the double occupation of the B-site (numbered in *italic*) cannot be detected due to the absence of long-range order, then the number of modes expected should be 10, in close agreement to the observed number. The spectra reflect therefore the general trends of the structural modifications disclosed by XRD.

As referred above, the main Bragg reflections observed in the solid solution can be indexed according to a simple perovskite structure. As can be visually detected, a similar situation is found in the IR reflectivity spectra, where four stronger reflectivity bands dominate. Fig. 3 depicts the values of the TO modes as function of the composition x , including the values of

the three IR active modes (F_{1u}) and the silent mode (F_{2u}) pertaining to pure ST (measured in a single crystal). As can be observed, the four more intense modes fitted to the composition $x=0.7$ ($\nu_1^{TO} = 112.8 \text{ cm}^{-1}$; $\nu_2^{TO} = 149.9 \text{ cm}^{-1}$; $\nu_3^{TO} = 195.3 \text{ cm}^{-1}$ and $\nu_4^{TO} = 253.8 \text{ cm}^{-1}$) can be related to a partial lift of the degeneracy of the two lower frequency F_{1u} modes of ST (A-BO₆ vibration and B-O₆ stretching¹²) caused by the lowering of the symmetry in the solid solution. Similarly, the higher frequency mode ($x=0.7$; $\nu_8^{TO} = 634.9 \text{ cm}^{-1}$) can be linked to the B-O₆ bending mode of ST. The secondary mode detected at $\nu_7^{TO} = 545.8 \text{ cm}^{-1}$ may be tentatively interpreted as due to the activation of the silent F_{2u} mode (B-O torsion) as a consequence of the symmetry breakdown. This assignment is consistent with the progressive suppression of this mode as x decreases down to $x=0.3$, which reflects the increase of the structural disorder in the lattice. Further decrease of the ST content induces a monoclinic structure and the splitting of modes at lower frequencies, as well as the appearance of additional weak modes. Some of these latter (located between 400 and 500 cm^{-1}) persist almost residually up to $x=0.7$.

Particularly interesting is the mode detected in LMT at about $\nu_{14}^{TO} = 543.5 \text{ cm}^{-1}$, the intensity of which decreases sharply as x increases to 0.1 and vanishes at $x < 0.3$. As in most $A(B_mB'_{1-m})O_3$ compounds with long range B-site order, the third lowest frequency corresponds to the extra B-B' stretching mode,¹³ hence we assign this mode to the Ti-Mg stretching. The increase of the intensity of this mode as $x \rightarrow 0$ may therefore be considered as a spectroscopic evidence of the onset of long-range B-site ordering in LMT.

The fit of the reflectivity spectra to the factorized form of the dielectric function allows us to evaluate, for the different compositions studied, the real and imaginary parts of dielectric function at IR frequency range (see Fig. 4). The dispersion observed reflects essentially the intrinsic contributions related to the dynamics of the lattice. At lower frequencies, other contributions to the dielectric response may arise due to extrinsic contributions such as porosity, second phase, grain boundaries and crystal defects. The parameters fitted to the IR spectra can therefore be used to estimate the relative importance of intrinsic (i.e. lattice related) contributions to the dielectric response at the microwave and radio-frequency ranges. The values of the permittivity of the different samples, evaluated at 0.26 cm^{-1} (8 GHz) from IR data, are shown in Table 2. Note that in the fit of IR spectra, TO and LO phonon frequencies are determined with a certain degree of accuracy which generally allows a good evaluation of the dielectric strengths of the polar modes. Hence, the extrapolated values of the permittivity of well processed ceramics are generally found to agree within errors of the order of 10% with those measured at MW

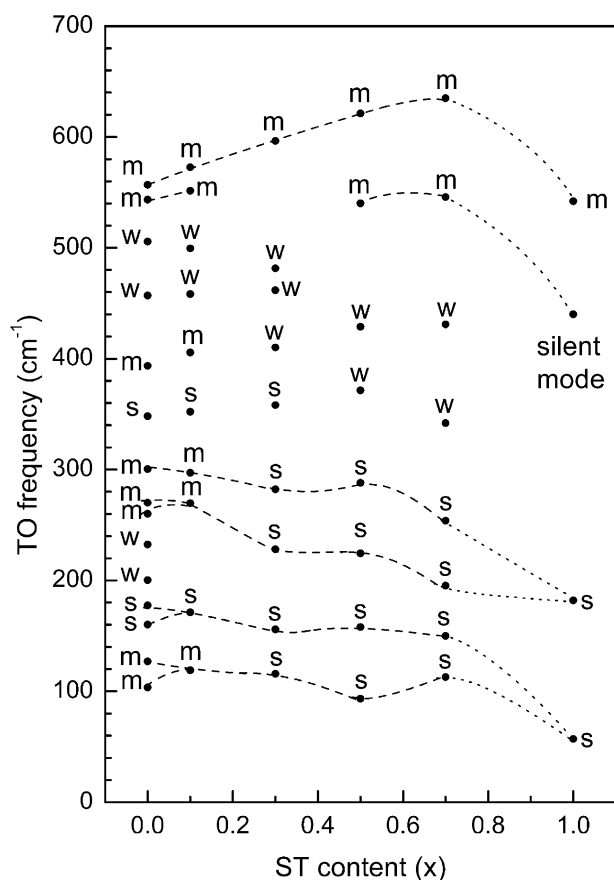


Fig. 3. Composition dependence of the TO phonon frequencies of the system $(1-x)\text{La}(\text{Mg}_{1/2}\text{Ti}_{1/2})\text{O}_3-x\text{SrTiO}_3$. The dielectric strength of each mode is indicated as strong (s), medium (m) or weak (w).

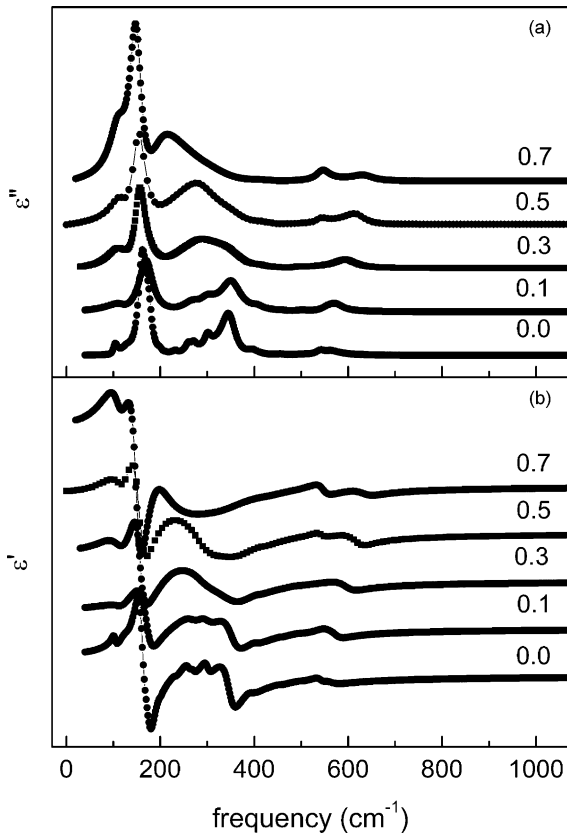


Fig. 4. Imaginary (a) and real components (b) of the dielectric function calculated from infrared reflectivity data for $(1-x)\text{LMT}-x\text{ST}$ samples. The numbers at the curves denote the x values.

Table 2

Dielectric characteristics of the $(1-x)\text{LMT}-x\text{ST}$ system determined at microwave range (MW), radio-frequencies (RF) and extrapolated from infrared (IR) data

x	MW				RF		IR	
	ϵ'	ϵ''	Q	f (GHz)	ϵ'	ϵ''	ϵ'	ϵ''
0	27.6	0.002	16110	7.10	26.3	0.009	28.6	0.002
0.1	29.2	0.014	2022	7.33	27.8	0.030	26.1	0.011
0.3	38.3	0.022	1763	6.59	34.0	0.044	38.2	0.014
0.5	48.1	0.045	1079	5.39	45.2	0.144	48.1	0.017
0.7	68.4	0.011	9913	5.41	62.0	0.141	73.3	0.036
0.9					118.0	0.307		

range. Contrary, the extrapolated losses are often less accurate.¹³

The temperature dependence of the low-frequency permittivity, measured in the vicinity of ambient temperature, showed no anomalies or dispersion in the range 10^2 – 10^6 Hz. As $\epsilon'(T)$ varies almost linearly, the thermal coefficient of capacitance (τ_C) was readily evaluated. The values of τ_f for the different ceramics were obtained from the low-frequency dielectric data by using the relation $\tau_f = 1/2[\tau_C + \alpha_L]$.³ The linear thermal-expansion coefficient (α_L) was assumed to be 10 ppm/K

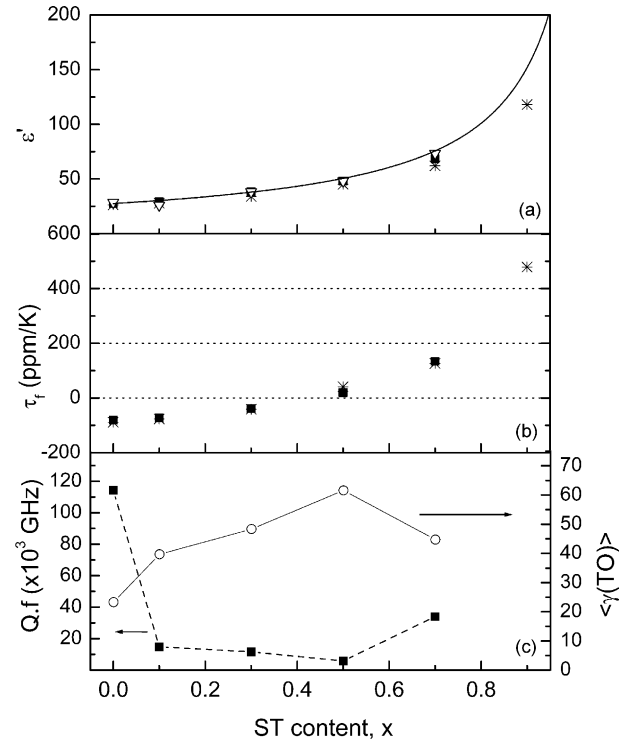


Fig. 5. Dielectric properties of the $(1-x)\text{LMT}-x\text{ST}$ system as a function of x : ϵ' (a), τ_f (b), $Q \cdot f$ value and average TO phonon damping, $\langle \gamma(\text{TO}) \rangle$, (c), measured at microwave (■), radio frequencies (*) and extrapolated from far infrared spectra (○).

because its value is found to be in the range 9–12 ppm/K for most perovskites.¹⁴

The relevant dielectric parameters, obtained by different methods on the $(1-x)\text{LMT}-x\text{ST}$ ceramics, are also presented in Fig. 5. The ϵ' values measured at microwave and radio frequencies exhibit a good agreement with those extrapolated from the FIR spectra (within an error less than 10%; Fig. 5a).

It has been observed^{15–17} that the compositional dependence of ϵ' in two-component dielectric mixture involving complex perovskites of the type $A(B_m B'_{1-m})\text{O}_3$ and CaTiO_3 or SrTiO_3 obeys to the empirical relationship:¹⁸

$$\frac{1}{\epsilon'(x)} = \frac{v_1}{\epsilon'_1} + \frac{v_2}{\epsilon'_2} \approx \frac{1-x}{\epsilon'_1} + \frac{x}{\epsilon'_2} \quad (1)$$

where v_i and ϵ'_i are the volume fraction and permittivity of the component i . The high relative density of the ceramics under study, absence of second phases and the small difference between unit cell volumes of end members (less than 2%), allow us to replace the volume fraction, v , by the molar fraction, x . As shown in Fig. 5a (solid line), the mixture rule expressed by Eq. (1) can describe rather well the compositional dependence of the permittivity, even if the ceramics are not simple mixtures but rather solid solutions with different symmetries.

Consider a solid solution with permittivity (ϵ'), average unit cell polarizability (α) and unit cell volume (V). As these quantities depend on the composition x , the

Clausius–Mossotti equation can be written as (ϵ_0 being the permittivity of vacuum):

$$\frac{\epsilon'(x) - 1}{\epsilon'(x) + 2} = \frac{\alpha(x)}{3\epsilon_0 V(x)} \quad (2)$$

Levin et al.¹⁹ used this equation to determine the compositional dependence of the macroscopic polarizability in the solid solutions $(1-x)\text{Ca}(\text{Al}_{1/2}\text{Nb}_{1/2})\text{O}_3 - x\text{CaTiO}_3$. Using their experimental data on $\epsilon'(x)$ and $V(x)$, they have shown that the polarizability varies nearly linearly with x , i.e. $\alpha(x) = (1-x)\alpha_1 + x\alpha_2$. Note, that the macroscopic polarizability α is not usually equal to the sum of the atomic polarizabilities of the atoms in the unit cell because of the crystalline field.²⁰ However, if the environment of all the atoms in the unit cell does not change fundamentally with x , as in the case of single-phase (perovskite) solid solutions, the crystal field effects do not influence much the dependence of $\alpha(x)$. The formation of single-phase perovskite solid solutions is known to be possible only if a difference in size of substituting atoms is not very large.²¹ Indeed, in the case of LMT–ST system, a small relative volume variation ($\Delta V/V < 2\%$) was determined. So, based on this one may consider $V_1 \approx V_2$. Taking into account that the permittivities of the end members are high enough, the above suppositions on $\alpha(x)$ and V allow to derive the “mixture rule” (Eq. 1) from the Clausius–Mossotti equation (Eq. 2).

It should be noted that this hyperbolic-type dependence (Eq. 1) for permittivity appears to be valid for solid solutions which involve high-permittivity dielectrics like “quantum paraelectrics” (SrTiO_3 , CaTiO_3) or even ferroelectrics below Curie point (BaTiO_3).² In this case the “dilution” of polarizability³ is the dominant mechanism controlling the permittivity and its thermostability coefficient, τ_e . If both end members have relatively low ϵ' (~ 30), the onset of oxygen octahedral tilt transition becomes an important factor affecting both ϵ' and τ_e .^{3,14,22}

As Fig. 5b shows, the values of τ_f measured at microwave and radio frequencies are in very good agreement for the whole set of LMT–ST samples studied. The function $\tau_f(x)$ follows a monotonic variation with x entirely analogous to that found in $\epsilon'(x)$. As can be seen, the value of τ_f is nearly zero at about $x \approx 0.40$. Several authors^{15,16} called the attention to the fact that the value $\tau_f \approx 0$ occurs at compositions x that are similar in various microwave dielectric solid solutions with SrTiO_3 and CaTiO_3 , despite the large difference observed in the values of τ_f . In the case of the $(1-x)\text{La}(\text{Zn}_{1/2}\text{Ti}_{1/2})\text{O}_3 - x\text{ATiO}_3$ ($A = \text{Sr}, \text{Ca}$) solid solutions, Cho et al.¹⁶ attributed this fact to the persistence of B-site ordering until $x = 0.5$, although this ordering was not obvious both from XRD and FIR data. According to our results, in the $(1-x)\text{LMT} - x\text{ST}$ system (Table 1, Figs. 2 and 3), this factor cannot be relevant as the cation ordering is lost for $x < 0.3$.

Fig. 6 shows the plot of τ_f vs ϵ' obtained from microwave ($x < 0.9$) and radio-frequency ($x = 0.9$) measurements. As shown, the function $\tau_f(\epsilon')$ is approximately linear in the full concentration range. According to Harrop,²³ the thermal coefficient of capacitance, τ_C , of paraelectric solid is often found to be proportional to ϵ' ($\tau_C = -\alpha_L \epsilon'$; α_L being the linear expansion coefficient). Since $\tau_f = 1/2[\tau_C + \alpha_L]$,³ it turns out that it must be a linear function of ϵ' , as observed in the LMT–ST system. Considering this empirical linear relation and Eq. (1), it can be easily proved that $\tau_f(x)$ must follow the relation:

$$\frac{1}{\tau_f(x)} = \frac{(1-x)\epsilon'_2 + x\epsilon'_1}{(1-x)\epsilon'_2\tau_1 + x\epsilon'_1\tau_2}, \quad (3)$$

where ϵ'_1, τ_1 and ϵ'_2, τ_2 represent the values of permittivity and temperature coefficient of the resonant frequency of the end members. Taking into account that the coefficients τ_f of the two end members have opposite sign, one can express the condition $\tau_f = 0$:

$$x(\tau_f = 0) = \left(1 - \frac{\epsilon'_1 \tau_2}{\tau_1 \epsilon'_2}\right)^{-1} \quad (4)$$

Note that $x(\tau_f = 0)$ is only a function of the ϵ'/τ_f ratio of end members. Using microwave dielectric data from Wise et al.³ for SrTiO_3 and CaTiO_3 , the ratio ϵ'/τ_f was found to be 0.176 and 0.188, respectively. According to Eq. 4, these similar values indicate that $\tau_f = 0$ must correspond to similar concentrations x in systems involving a negative- τ_f compounds and CaTiO_3 or SrTiO_3 . In the case of $(1-x)\text{LMT} - x\text{ST}$ system, Eq. 4 gives the value $x(\tau_f = 0) \approx 0.36$, which is in good agreement with the experimental result.

The quality factor of the different samples investigated, expressed by the product $Q \cdot f$, is shown in Fig. 5c as function of x . As x increase, $Q \cdot f$ shows a sharp

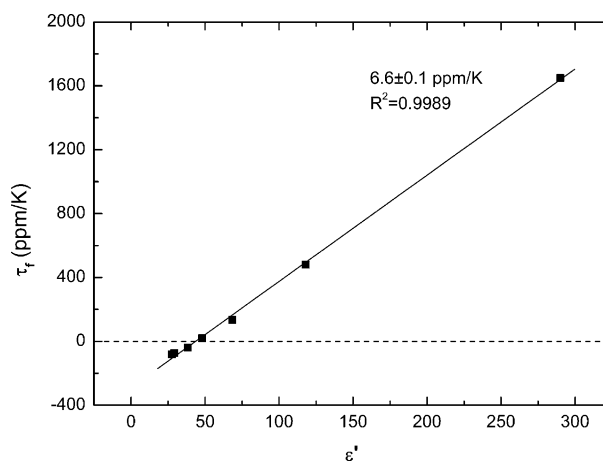


Fig. 6. τ_f versus ϵ' for the $(1-x)\text{LMT} - x\text{ST}$ system (for composition of $x = 1$ the data were adopted from Ref. 3). The line slope, $\Delta\tau_f/\Delta\epsilon'$, is presented on the plot.

decrease at $x=0.1$, followed by small variation for intermediate compositions ($0.3 < x < 0.7$). Some authors¹⁶ related the decrease of $Q \cdot f$ in mixed systems with ordered $A(B_m B'_{1-m})O_3$ compounds to the loss of cation ordering. In the LMT–ST ceramics, the XRD and IR results show that the degree of ordering is already strongly reduced at $x=0.1$. The observed decrease of $Q \cdot f$ at $x=0.1$ is therefore consistent with this hypothesis. Note, however, that either intrinsic (i.e. lattice related²⁴) or extrinsic mechanisms can be at the origin of such a reduction of the $Q \cdot f$ value. In the case of LMT–ST system intrinsic mechanisms seem to dominate. As can be seen in Fig. 5c, the compositional dependence of the weighted sum of TO phonon damping, $\langle \gamma(\text{TO}) \rangle = \sum_{j=1}^n \gamma_j(\text{TO}) \Delta \varepsilon_j / \sum_{j=1}^n \Delta \varepsilon_j$ (γ_j and $\Delta \varepsilon_j$ represent the values of damping and dielectric strength of j -th mode) correlates well with $Q \cdot f(x)$, suggesting that $Q \cdot f(x)$ dependence in the $(1-x)\text{LMT}-x\text{ST}$ system follows essentially the average anharmonicity of the crystal lattice.

4. Conclusion

Dense, homogeneous and single-phase perovskite ceramics $(1-x)\text{La}(\text{Mg}_{1/2}\text{Ti}_{1/2})\text{O}_3-x\text{SrTiO}_3$ were processed from powders obtained by a nonconventional chemical route, based on the Pechini method. These ceramics were dielectrically characterized at radio, microwave and far infrared (FIR) frequency regions. The FIR spectra reflect the sequence of structure transformations revealed by X-ray diffraction. The values of the dielectric permittivity, measured at room temperature, in the microwave and radio-frequency ranges were found to agree with the values extrapolated from FIR data. The dependences of the dielectric permittivity (ε') and temperature coefficient of the resonant frequency (τ_f) on composition follow mixture-like laws. The composition where τ_f changes sign has been estimated to be close to $x=0.40$. The results of the dielectric characterization indicate that the dependences of both $\varepsilon'(x)$ and $\tau_f(x)$ reflect more the dilution of average ionic polarizability than the onset of an oxygen octahedra tilt transition. The obtained values of permittivity and quality factor ($Q \cdot f$) as well as their compositional dependences testify the microwave dielectric response of the $(1-x)\text{La}(\text{Mg}_{1/2}\text{Ti}_{1/2})\text{O}_3-x\text{SrTiO}_3$ ceramics is dominated by lattice related mechanisms.

Due to the relatively high permittivity (~ 45) and the potential ability to tune the value of τ_f , the $\text{La}(\text{Mg}_{1/2}\text{Ti}_{1/2})\text{O}_3\text{--SrTiO}_3$ mixed system seems to be a promising technological material for microwave applications. Efforts are presently being made to improve the values of the quality factor.

Acknowledgements

The authors thank Mr. R.C. Pullar and Professor N.McN. Alford for the help with some of the microwave dielectric measurements. The authors also acknowledge the Foundation for Science and Technology (FCT-Portugal) for their support (Project POCTI/40187/CTM/2001).

References

1. Cava, R. J., Dielectric materials for applications in microwave communications. *J. Mater. Chem.*, 2001, **11**, 54–65.
2. Seabra, M. P., Salak, A. N., Avdeev, M. and Ferreira, V. M., $\text{La}(\text{Mg}_{1/2}\text{Ti}_{1/2})\text{O}_3$ -based materials for microwave applications. *Key Engineering Materials* (accepted for publication).
3. Wise, P. L., Reaney, I. M., Lee, W. E., Iddles, D. M., Cannell, D. S. and Price, T. J., Tunability of τ_f in perovskites and related compounds. *J. Mater. Res.*, 2002, **17**, 2033–2040.
4. Avdeev, M., Seabra, M. P. and Ferreira, V. M., Structure evolution in $\text{La}(\text{Mg}_{0.5}\text{Ti}_{0.5})\text{O}_3\text{--SrTiO}_3$ system. *Mat. Res. Bull.*, 2002, **37**, 1459–1468.
5. Seabra, M. P. and Ferreira, V. M., Synthesis of $\text{La}(\text{Mg}_{0.5}\text{Ti}_{0.5})\text{O}_3$ ceramics for microwave applications. *Mat. Res. Bull.*, 2002, **37**, 255–262.
6. Hakki, B. W. and Coleman, P. D., A dielectric resonator method of measuring inductive capacities in the millimeter range. *IRE Trans Microwave Theory and Tech.*, 1960, **8**, 402–410.
7. Kajfez, D. and Guillion, P., *Dielectric Resonators*. Artech House, Zurich, Switzerland, 1986.
8. Berreman, D. W. and Unterwald, F. C., Adjusting poles and zeros of dielectric dispersion to fit reststrahlen of PrCl_3 and LaCl_3 . *Phys. Rev.*, 1968, **174**, 791–799.
9. Ferreira, V. M., Azough, F., Baptista, J. L. and Freer, R., Magnesium titanate microwave dielectric ceramics. *Ferroelectrics*, 1992, **133**, 127–132.
10. Penn, S. J., Alford, N. McN., Templeton, A., Wang, X., Xu, M., Reece, M. and Schrapel, K., Effect of porosity and grain size on the microwave dielectric properties of sintered alumina. *J. Amer. Ceram. Soc.*, 1997, **80**, 1885–1888.
11. Rousseau, D. L., Bauman, R. P. and Porto, S. P. S., Normal mode determination in crystals. *J. Raman Spectroscopy*, 1981, **10**, 253–290.
12. Gervais, F., Origin of ferroelectricity in highly-polar oxides: small changes of chemical bonding enhanced by local electric field. *Jpn. J. Appl. Phys.*, 1985, **24**, 198–200.
13. Zurmühlen, R., Petzelt, J., Kamba, S., Voitsekhovskii, V., Colla, E. and Setter, N., Dielectric spectroscopy of $\text{Ba}(\text{B}'_{1/2}\text{B}''_{1/2})\text{O}_3$ complex perovskite ceramics correlations between ionic parameters and microwave dielectric properties. I. Infrared reflectivity study (10^{12} – 10^{14} Hz). *J. Appl. Phys.*, 1995, **77**, 5341–5350.
14. Colla, E. L., Reaney, I. M. and Setter, N., Effect of structural changes in complex perovskites on the temperature coefficient of the relative permittivity. *J. Appl. Phys.*, 1993, **74**, 3414–3425.
15. Cho, S.-Y., Kim, I.-T. and Hong, K. S., Crystal structure and microwave dielectric properties of $(1-x)\text{La}(\text{Zn}_{1/2}\text{Ti}_{1/2})\text{O}_3-x\text{SrTiO}_3$ system. *Jpn. J. Appl. Phys.*, 1998, **37**, 593–596.
16. Cho, S.-Y., Youn, H.-J., Lee, H.-J. and Hong, K. S., Contribution of structure to temperature dependence of resonant frequency in the $(1-x)\text{La}(\text{Zn}_{1/2}\text{Ti}_{1/2})\text{O}_3-x\text{ATiO}_3$ ($A = \text{Ca}, \text{Sr}$) system. *J. Amer. Ceram. Soc.*, 2001, **84**, 753–758.
17. Kucheiko, S., Choi, J.-W., Kim, H.-J. and Jung, H.-J., Microwave dielectric properties of $\text{CaTiO}_3\text{--Ca}(\text{Al}_{1/2}\text{Nb}_{1/2})\text{O}_3$ ceramics. *J. Amer. Ceram. Soc.*, 1996, **79**, 2739–2743.

18. Kingery, W. D., *Introduction to Ceramics*. John Wiley & Sons, New York, 1976.
19. Levin, I., Chan, J. Y., Maslar, J. E., Vanderah, T. A. and Bell, S. M., Phase transitions and microwave dielectric properties in the perovskite-like $\text{Ca}(\text{Al}_{0.5}\text{Nb}_{0.5})\text{O}_3$ – CaTiO_3 system. *J. Appl. Phys.*, 2001, **90**, 904–913.
20. Wersing, W., High frequency ceramic dielectrics and their application for microwave components. In *Electronic Ceramics*. Elsevier, London & New York, 1991, pp. 67–119.
21. Dergunova, N. V. and Geguzina, G. A., The isomorphism conditions in complex oxides with perovskite structure. *Isv. Akad. Nauk SSSR, ser. fiz.*, 1990, **54**, 1212–1214 (in Russian).
22. Reaney, I. M., Colla, E. L. and Setter, N., Dielectric and structural characteristics of Ba- and Sr-based complex perovskites as a function of tolerance factor. *Jpn. J. Appl. Phys.*, 1994, **33**, 3984–3990.
23. Harrop, P. J., Temperature coefficients of capacitance of solids. *J. Mater. Sci.*, 1960, **4**, 370–374.
24. Seabra, M. P., Salak, A. N., Avdeev, M. and Ferreira, V. M., Structure and dielectric characterization of the $\text{La}(\text{Mg}_{1/2}\text{Ti}_{1/2})\text{O}_3$ – $\text{Nd}(\text{Mg}_{1/2}\text{Ti}_{1/2})\text{O}_3$ system. *J. Phys.: Condens. Matter.*, 2003, **15**, 4229–4238.